Characterizing the combined effects of force, repetition and posture on injury pathways and micro-structural damage in isolated functional spinal units from sub-acute-failure magnitudes of cyclic compressive loading

Chad E. Gooyers [1], Elliott M. McMillan, Mamiko Noguchi, Joe Quadrilatero, Jack P. Callaghan *

Department of Kinesiology, Faculty of Applied Health Sciences, University of Waterloo, Waterloo, ON, Canada, N2L 3G1

ARTICLE INFO

ABSTRACT

Background: Previous research suggests that when the magnitude of peak compressive force applied during cyclic loading exceeds 30% of a functional spinal unit's estimated ultimate compressive tolerance, fatigue failure of the cartilaginous endplate or vertebra will occur before intervertebral disc herniation.
Methods: Three levels of peak compressive force, three cycle rates and two dynamic postural conditions were examined using a full-factorial design. Cyclic compressive force was applied using a modified material testing apparatus, in accordance with a biofidelic time-varying waveform with synchronous flexion/extension rotation for 5000 cycles. Annulus fibrosus tissue from 36 "survivor" FSUs was excised for histological analysis.
Results: 80% of specimens survived 5000 cycles of cyclic loading. A marked difference of the magnitude of peak compressive force was noted in the Kaplan–Meier survival function of experimental conditions that induced fatigue injury. Overall, in the 40% ultimate compressive tolerance load condition, the probability of survival was less than 67%. The micro-structural damage detected in excised samples of annulus fibrosus tissue consisted of clefts and fissures within the intra-lamellar matrix, as well as delamination within the inter-lamellar matrix.
Interpretation: Consistent with previous research, our findings support a threshold of peak compressive force of 30% ultimate compressive tolerance, where cyclic loading above this level will likely result in fatigue injury in less than 5000 cycles of *in vitro* mechanical loading. However, findings from our histological analyses demonstrate that considerable micro-structural damage occurred in specimens that "survived" the cyclic loading exposure.

© 2015 Elsevier Ltd. All rights reserved.

1. Introduction

Previous epidemiological studies have identified a link between cumulative exposure to mechanical load and the reporting of low back pain and injury (Coenen et al., 2013; Kumar, 1990; Norman et al., 1998; Seidler, 2001, 2003). As such, numerous *in vitro* studies have been conducted to explore lumbar spine injury pathways in response to cyclic loading (Adams and Hutton, 1983; Brinckmann and Hilweg, 1989; Brinckmann et al., 1988; Callaghan and McGill, 2001; Gallagher et al., 2005; Gooyers et al., 2013; Hansson et al., 1987; Howarth and Callaghan, 2013; Parkinson and Callaghan, 2007a,b, 2008, 2009). Since cumulative mechanical exposure is influenced by several factors, including: the magnitude of the applied force, frequency of repetition (i.e. cycle rate), duration of the exposure cycle, and joint posture, each

of these factors have been closely studied to examine their influence on injury mechanisms in the osteoligamentous tissues that comprise the intact spine (e.g. vertebrae, intervertebral disc, cartilaginous endplate, ligaments, joint capsule, etc.).

Depending on the loading profile that is adopted for testing, common injury mechanisms linked to cyclic loading in the lumbar spine include: vertebral fracture (Brinckmann et al., 1988; Hansson et al., 1987; Liu et al., 1983), failure of the cartilaginous endplate (Brinckmann and Hilweg, 1989; Gallagher et al., 2005; Parkinson and Callaghan, 2007a, 2009), intervertebral disc (IVD) disruption (e.g. herniation) (Callaghan and McGill, 2001; Tampier et al., 2007) and fracture of the pars interarticularis (Howarth and Callaghan, 2013). Research conducted by Parkinson and Callaghan (Parkinson and Callaghan, 2009) identified that when the magnitude of peak compressive force applied during cyclic loading exceeds 30% of a functional spinal unit's (FSU) estimated ultimate compressive tolerance (UCT), endplate fracture will occur before IVD herniation, as long as the range of dynamic flexion/extension does not exceed the normal physiologic joint range. This is consistent with earlier research conducted by Brinckmann et al. (Brinckmann et al., 1988), which found that most FSUs could tolerate 5000 cycles of

* Corresponding author at: Department of Kinesiology, Faculty of Applied Health Sciences, University of Waterloo, Waterloo, Ontario, N2L 3G1, Canada.
E-mail address: callagha@uwaterloo.ca (J.P. Callaghan).
[1] Present Address: Giffin Koerth Forensic Engineering & Science, 40 University Avenue, Toronto, ON M5J 1T1.

cyclic compressive at loads below 30% UCT. However, the amount of tissue damage imposed to the IVD of "survivor" specimens from these investigations remains unknown, as this threshold is limited by the gross radiographic measures that were applied to track the migration of the nucleus pulposus in the IVD (Parkinson and Callaghan, 2009) or sudden changes in specimen displacement during a loading cycle (Brinckmann and Hilweg, 1989; Brinckmann et al., 1988; Hansson et al., 1987). This was followed by subsequent analysis of macroscopic damage by cutting through the IVD and inspecting each vertebrae.

Therefore, the primary objective of this study was to explore the combined effects of: (i) the magnitude of the peak compressive force, (ii) cycle rate and (iii) degree of postural deviation on known injury pathways in isolated FSUs at sub-acute-failure magnitudes of peak compressive force. A secondary objective was to characterize the micro-structural damage imposed to IVDs in "survivor" specimens using histological methods.

2. Methods

2.1. Specimen preparation

The cervical spines of 63 porcine specimens (mean age = 6 months, weight = 85 kg) were obtained following death and stored at −20 °C. Each cervical spine was separated into two FSUs for *in vitro* mechanical testing, which included two vertebrae and the IVD at the c34 and c56 level; resulting in a total of 126 FSUs. Porcine cervical FSUs were used as surrogates for the human lumbar spine due to their anatomical and functional similarities (Oxland et al., 1991; Yingling et al., 1999), providing superior control over potential confounding factors (e.g. age, nutrition, physical activity) that can impact the mechanical integrity of the tissues surrounding the intervertebral joint. This was important for the histological analyses performed in this study, as the microstructural damage observed could then be linked to the mechanical loading exposure and not be confounded by prior degeneration and tissue damage that is commonly observed in elderly human cadaveric tissue.

The inclusion criteria required that FSUs met a non-degenerated disc quality (Grade 1) as outlined by Galante (1967). Before testing, frozen specimens were thawed at room temperature for a minimum of 12 h. Dissection of the cervical spine involved isolating the two FSUs of interest (i.e. c34, c56) and carefully removing the surrounding musculature leaving only the osteoligamentous structures intact, except for the portion of the anterior longitudinal ligament that attached to the anterior surface of the AF, which was removed to expose the IVD for surface measurements. Once the dissection protocol was complete, width and depth measurements of the two exposed endplates (superior and inferior) were recorded using digital calipers. These measurements were used to estimate the endplate surface area of the intact intervertebral joint using the equation of an ellipse, which was then used to predict each FSU's UCT without destructive testing (Parkinson et al., 2005). This method enabled normalization of peak cyclic compression across specimens.

Before mounting each FSU for testing, the anterior processes and exposed facets were trimmed to ensure the exposed cartilaginous endplates were responsible for load carriage at the interfaces with the testing system. Next, the FSU was fixed within custom-machined aluminium cups using a combination of wood screws (fixed approximately 1 cm into the centre of the exposed endplates) and non-exothermic dental plaster (Denstone; Miles, Southbend, IN, USA). To prevent specimen dehydration throughout the dissection and potting procedures, all FSUs were misted with a saline solution (0.9% weight per volume) approximately every 15 min.

2.2. Procedure

The potted specimens were then mounted in a servo-hydraulic materials testing system (Model 8872; Instron, Canton, MA, USA) that

has been modified to apply flexion/extension rotations to FSUs under compressive load. The testing jig was designed to allow the centre of rotation to be aligned (vertically and horizontally) with the geometric centre of the IVD (Callaghan and McGill, 2001). The lower vertebra of each test specimen was free to translate in the anterior-posterior and medial-lateral direction (via a bearing tray), which enabled the centre of rotation to translate within the joint during loading. To minimize dehydration during mechanical testing, FSUs were covered with saline soaked gauze and plastic wrap.

Each FSU initially received 15 min of static compressive force (300 N) to counter any postmortem swelling that occurred within the IVD (Callaghan and McGill, 2001). This load has previously been identified to equilibrate specimen height, without inducing excessive creep over a period of 15 min. During this preload test, an independent brushless servomotor (AKM23D; Kollmorgen/Danaher Motion, Radford, VA, USA) connected in-series with a torque cell (T120-106-1K; SensorData Technologies Inc., Sterling heights, MI, USA) was used to establish the angular position of minimal stiffness about the flexion/extension axis. Following the preload test, three cycles of passive flexion–extension (PFE) joint rotations were applied (0.5° per second) to identify the limits of each FSU's flexion/extension neutral zone. Using custom software, interfaced with an ISA bus motion controller (Model DMC18x0, Galil Motion Control, Rocklin, CA USA), the applied moment and angular displacement were sampled at 25 Hz. The flexion and extension limits of the neutral zone were identified using methods described by Thompson et al. (Thompson et al., 2003); whereby the first-derivative of a fourth-order polynomial fit to moment-angle data from the last two loading cycles was used to detect the angular displacement where this function deviates from linear. These neutral zone limits were used to establish the dynamic range of flexion/extension rotation that was applied during cyclic testing (Fig. 1).

Upon completion of both the preload and PFE tests, specimens were randomly assigned to 1 of 18 experimental conditions (7 FSUs per group). Three levels of peak compressive force (10, 20 and 40% of specimens' ultimate compressive tolerance; UCT), three cycle rates (5, 10 and 30 cycles per minute) and two dynamic postural conditions, including: (i) 100% neutral zone range; average (SD) of 6.79° (2.23) and (ii) 300% neutral zone range; 20.52° (4.41), were examined using a full-factorial design. The 100% neutral zone postural condition was intended to represent a lifting technique with sound mechanics (i.e. minimal lumbar spine motion), whereas the 300% condition was designed to bring the isolated joint to the end of its natural physiological range (i.e. where the passive flexion rotational stiffness begins to deviate from linear). Compressive force was applied in accordance with a biofidelic, time-varying waveform (two-seconds duration) that was based on the *in vivo* estimate of compressive loading in the lumbar spine during an occupation lifting task using a dynamic EMG-assisted musculoskeletal model (Parkinson et al., 2011). The applied compressive
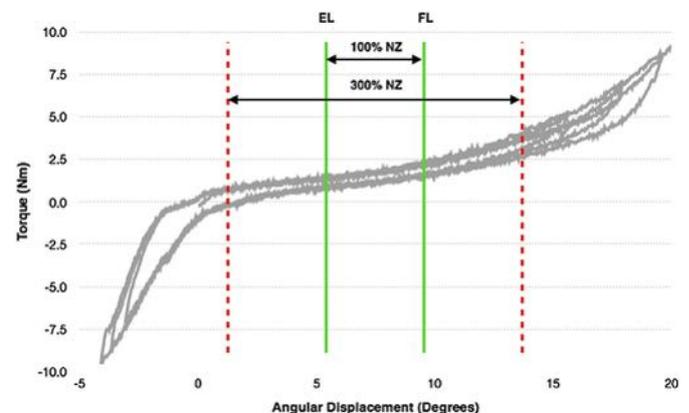

Fig. 1. Sample passive flexion/extension test. (NZ = neutral zone; FL = flexion limit; EL = extension limit).

force was scaled to run from a minimum of −0.001 N to the desired peak load (i.e. 10, 20, and 40% of each FSU's predicted UCT). Similar to research conducted by Parkinson and Callaghan (2009), dynamic flexion/extension was synchronously applied during each loading cycle using a motion profile recorded from the lumbar spine during the same floor to waist height lift, and was scaled for each posture condition to 100 and 300% of the specimens' neutral zone range. Specimens were kept in a neutral posture between loading cycles. However, it is important to note that the applied compressive force is not the load that is experienced across the intact vertebral joint, except in a neutral posture, as this force is partitioned into compressive and shear components through the testing jig (dependent on joint angle), the same as what would occur in the *in vivo* spine in the absence of muscle force.

All FSUs were cyclically loaded for 5000 cycles or until failure occurred, which was identified by specimen height loss greater than 9 mm (Parkinson and Callaghan, 2009). Throughout testing, measurements of the applied compressive force and vertical position of the Instron actuator were sampled at 32 Hz using a 16-bit analog-to-digital conversion board (National Instruments, Austin, TX, USA), which enabled post-test determination of the exact loading cycle in cases of where endplate/bone failure occurred. The fracture cycle was identified by a change in average cycle compressive stiffness, calculated using single cycle displacement measures at the instance of peak loading (Parkinson and Callaghan, 2007a), as well as a precipitous drop in specimen height (Brinckmann and Hilweg, 1989; Hansson et al., 1987; Parkinson and Callaghan, 2009) and a concomitant change in the applied sagittal-plane torque

Upon completion of the mechanical testing protocol, AF tissue from 36 randomly selected "survivor" FSUs (18 c34, 18 c56; two per experimental condition) was excised for histological analysis. Three tissue samples (4 × 4 mm), consisting of the outermost 10 lamellae (approximately 2 mm thick) were obtained from both the anterior and posterior–lateral regions of the IVD (6 total) from each specimen. Additional tissue samples were obtained from two control specimens (1 c34, 1 c56) that underwent the same preloading protocol but were not subjected to the cyclic loading exposure. These specimens enabled a comparison of the potential micro-structural damage imposed from sectioning alone, compared to that induced by the cyclic mechanical loading exposure. Each sample was embedded in Tissue-Tek OCT (Optimum Cutting Temperature; Sakura Finetek, Torrance, CA, USA) compound and then rapidly frozen in liquid nitrogen and stored at −80 °C until sectioning.

2.3. Histological analyses

To characterize the micro-structural damage in the AF, frozen tissue samples mounted in OCT compound were serially sectioned in the frontal and transverse planes using a cryostat microtome. A total of 54 tissue sections from each specimen, obtained from the anterior and posterior–lateral regions of the IVD (in each plane) were mounted onto Vectabond coated (Vector Laboratories, Burlingame, CA, USA) glass microscope slides and air dried for 5 min. Eighteen 10 μm sections were cut from the superficial (9 anterior, 9 posterior–lateral) and deep layers (9 anterior, 9 posterior–lateral). An additional 18 sections were cut in the transverse plane across all layers of the sample (9 anterior, 9 posterior–lateral). The sections were then stained with haematoxylin and eosin (H&E) and visualized using a brightfield microscope (Nikon Instruments Inc., Melville, NY, USA) linked to a digital camera (PixeLink, Ottawa, ON, Canada).

The H&E staining protocol consisted of: (i) immersing each tissue section in hemaetoxylin for 60 seconds, (ii) rinsing the glass microscope slide in tap water (10×, repeated 1-second submersion), (iii) counter-staining with eosin for 90 s, (iv) 5×, 1-second submersion in 70% ethanol, (vi) 5×, 1-second submersion in 95% ethanol, (vii) 5×, 1-second submersion in 100% ethanol and (viii) 5×, 1-second submersion in Xylene. Lastly, the tissue sections were air-dried and mounted in

Permount (Fischer Scientific Co., Fair Lawn, NJ, USA) with a #2 coverslip. Characteristic images from each specimen were captured at 10× magnification (2048 × 1536 RGB image resolution) using Image-Pro Plus analysis software (Media Cybernetics, Silver Spring, USA). Qualitative analysis of micro-structural damage was assessed across: (i) magnitude of peak compressive force (10% UCT, 20% UCT), (ii) cycle rate (5, 10 and 30 cycles per minute), (iii) degree of postural deviation (100% vs. 300% NZ range) and (iv) radial location on the IVD (anterior vs. posterior–lateral).

Since the cyclic loading protocol was not immediately stopped when an endplate fracture occurred, it was not possible to conduct controlled histological comparisons of the disruption imposed to the IVD across specimens assigned to the 40% UCT loading conditions since they were exposed to a different number of loading cycles and cumulative compression. In addition, evidence of non-physiological freezer damage emerged in some stained tissue sections, potentially due to post-mortem freezing and/or flash freezing in OCT compound with liquid nitrogen. This damage was characterized by a clear circular pattern of disruption in the intra-lamellar matrix, easily distinguishable from naturally occurring damage to the matrix, and if present the specimen was excluded from our analysis. As such, tissue samples from three specimens were excluded from the study.

2.4. Statistical analyses

Due to technical difficulties in synchronizing the cyclic compressive load with the flexion/extension axes, three FSUs were excluded from the analyses presented, resulting in a total sample of 123 specimens included in the study. All statistical analyses were computed using SAS software (version 9.2, SAS Institute Inc., Cary, NC) with a significance level (α) of 0.05 set *a priori*. Specimen randomization was assessed using a three-way (force, cycle rate and postural deviation) general linear model (GLM) to test for group differences in the estimated endplate area (mm^2) of the intact joint or neutral zone range (degrees) across experimental conditions. The Kaplan–Meier estimator was used to estimate the survival function for each experimental condition (Kaplan and Meier, 1958).

3. Results

3.1. Specimen randomization

Successful randomization across experimental conditions was achieved, as no significant main effects of force, cycle rate or postural deviation were revealed in estimates of endplate area ($p > 0.3104$) or neutral zone range ($p > 0.6744$). Interestingly, there were also no significant differences in estimates of endplate area ($p = 0.3065$) or neutral zone range ($p = 0.6525$) between failed specimens compared with those that survived the cyclic mechanical exposure.

3.2. Fatigue injury

Of the 123 specimens that were considered for analysis, 99 (80%) survived 5000 cycles of cyclic compressive loading. Twenty-four FSUs experienced a fatigue-related injury, which could be classified into three primary injury pathways: (i) endplate fracture (Fig. 2A), (ii) avulsion of the superior cartilaginous endplate on the anterior border of the vertebrae (Fig. 2B) and (iii) fracture of the pars interarticularis (Fig. 2C). A summary of the distribution of all 24 specimens across each injury mechanism is provided in Table 1. Interestingly, 23/24 of the fatigue related injuries occurred in the 40% UCT experimental conditions. There were no fatigue injuries observed in the 10% UCT group and only one FSU (c56; 10 cycles per minute, 300% neutral zone range) exhibited a fracture of the pars interarticularis in the 20% UCT condition. Half of all fatigue-related injuries (12/24) were endplate fractures, of which 11 occurred in the caudal endplate of the superior vertebrae. Although there
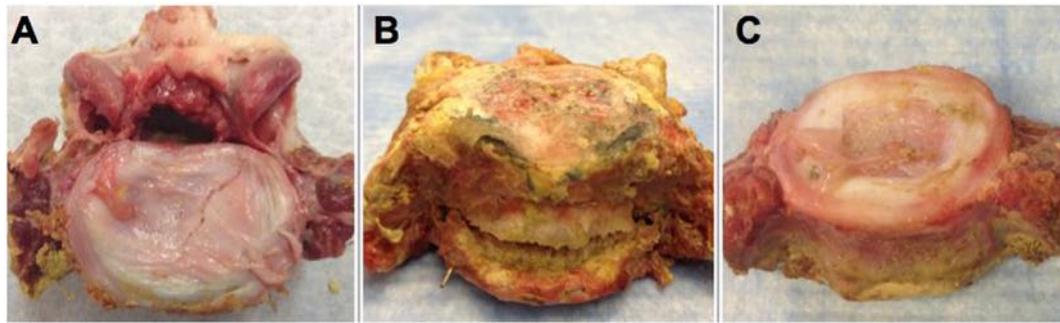
Fig. 2. Classification of fatigue failure injury mechanisms: (A) Cartilaginous endplate fracture, (B) avulsion of the superior endplate, and (C) fracture of pars interarticularis (posterior elements removed).

were 8 avulsions of the cranial endplate from the inferior vertebra, this mechanism of failure only occurred in the 300% neutral zone range conditions. When analyzed by cycle rate, it is noteworthy that over 40% (10/24) of all fatigue injuries were observed in the 5 cycles per minute condition.

3.3. Survival analysis

A marked difference in the magnitude of peak compressive force was noted in the survival function between experimental conditions that induced fatigue injury in less than 5000 cycles, with a higher survivorship at 20% UCT (Fig. 3). However, within the 40% UCT group there were no detectable differences across cycle rate and posture conditions, depicted by several intersections in the Kaplan-Meier survival functions. It is noteworthy that across all 40% UCT loading groups, the probability that specimens will survive 5000 cycles of cyclic compressive loading was less than 67%.

3.4. Histological analysis

The micro-structural damage observed in excised samples of AF tissue that underwent cyclic loading consisted of clefts and fissures within the intra-lamellar matrix, as well as delamination within the inter-lamellar matrix. This was not observed in the control specimens (Fig. 4). Representative images of the disruption observed in the intra-lamellar matrix from the anterior and posterior–lateral regions of the IVD are presented in Figs. 5 and 6 respectively. Damage observed between layers in the AF is depicted in Fig. 7. There was no consistent trend in the amount of damage that was observed between 10% and 20% UCT loading conditions. However, a noticeable effect of posture was observed across some conditions, with increased damage in tissue samples from the 300% NZ range condition. As expected, tissue samples excised from the posterior–lateral region were also found to have more disruption (i.e. clefts, fissures, etc.), in comparison to those excised from the anterior region of the IVD. Similarly, a trend emerged that more

disruption was observed in sections obtained from deeper layers of the IVD. When considering the representative images across each of the 10 and 20% UCT experimental conditions, it is noteworthy that a qualitative depiction of emerging interactions could be detected. For example, in the representative images from tissue samples harvested from the posterior–lateral region of the IVD, comparable micro-structural damage can be seen in superficial layers from specimens assigned to the 10% UCT force condition at 5 cycles per minute (300% neutral zone) to those in same 10% UCT force condition but applied at 30 cycles per minute (100% neutral zone).

4. Discussion

Consistent with our hypothesis, the mode of specimen failure was altered across each of the different loading conditions that were examined in this study. Despite the fact that 80% of specimens "survived" 5000 cycles of cyclic loading, there was considerable micro-structural damage observed in the AF, with increased disruption in the deeper layers of the AF, and in those samples excised from the posterior–lateral region of the IVD. This observation challenges the recent theory proposed by Wade et al. (Wade et al., 2014), that damage in ovine lumbar motion segments is initiated in the mid-then-outer annulus, as a consequence of the higher strain burden in this region from endplate curvature. Nonetheless, the magnitude of postural deviation was found to have the greatest influence on the amount of micro-structural disruption imposed to the AF.

The frequency of macroscopic fatigue injury observed across each of the different experimental conditions is consistent with previous research. For example, using a similar loading protocol, Parkinson and Callaghan (2009) showed that when the magnitude of peak compressive force exceeded 30% of a FSU's estimated UCT, endplate fracture will occur before IVD herniation. Although specimens included in their study were exposed to a maximum of 21,600 cycles (baseline static compressive load of 300 N), the average (SD) injury cycle for the 10% and 30% UCT loading groups were 14,400 (6859) and 5031 (3944), respectively, with no significant differences in the cumulative compression to failure. This is in agreement with the results from the present study with only one fatigue injury documented in the 20% UCT group (after 4303 cycles). Collectively, our results provide strong support for the existence of a non-linear relationship between the magnitude of peak compressive force and the risk of fatigue injury in isolated FSUs, particularly for the cartilaginous endplates.

When considering the distribution and type of injuries that were documented in this study, a significant effect of postural deviation was found. Specifically, specimens exposed to dynamic flexion/extension to a range of 300% of their neutral zone experienced either a fracture of the pars interarticularis of the superior vertebrae or avulsion of the superior endplate. A known mechanism for fatigue fracture of the pars interarticularis is repetitive hyperextension (Standaert and Herring, 2000). Similarly, avulsion of the cartilaginous endplate at the anterior border of the vertebrae has been linked to forceful hyperextension

Table 1
Distribution of fatigue injury across experimental conditions.

Force (%UCT)	Repetition (cycles/min)	Posture (% NZ)	Injury frequency				Total
			EF	EA	PF	M	
20	10	300				1	1
40	5	100	7				7
40	5	300		3			3
40	10	100	2				2
40	10	300	2	2		2	6
40	30	100					0
40	30	300	1	3		1	5
Total			12	8	1	3	24

Note: EF = endplate fracture EA = endplate avulsion PF = pars fracture M = mixed; combination of EF & EA.
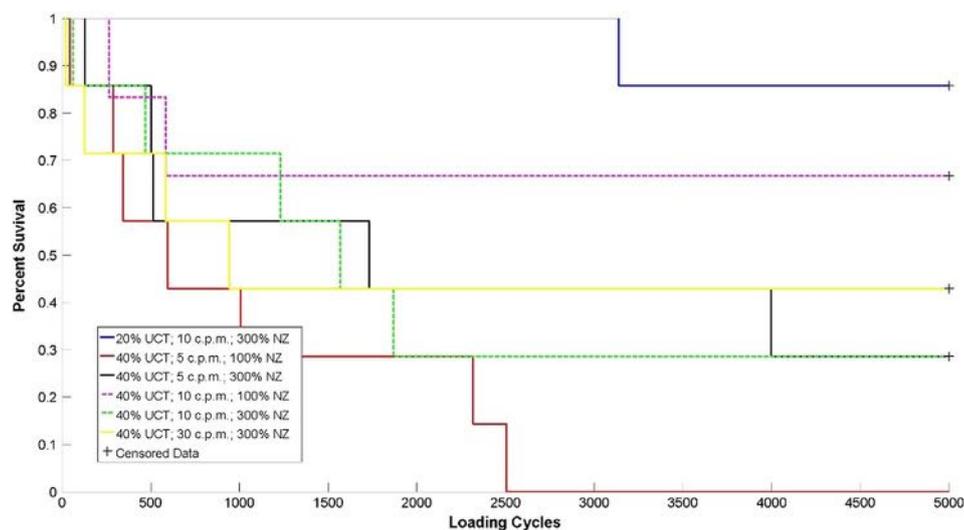
Fig. 3. Kaplan–Meier survival analysis across cyclic loading conditions that induced fatigue injury. Note that the survival function of all other experimental conditions (not shown on the graph) would be a horizontal line with a y-intercept equal to 1.

(Denis and Burkus, 1992). However, it should be acknowledged that the porcine FSUs included in the study were skeletally immature and that previous research using the same porcine animal model has noted endplate avulsion injuries with cyclic compressive loading (Tampier et al., 2007). Yingling et al. (1997) also noted a similar mechanism of injury with compression loading at high load rates, which was attributed to weak bony attachment of the AF to the vertebral body compared to the strength of the collagenous fibers of the AF, which ultimately lead to rupture of the annulus-bone interface. Therefore, since it is likely that the cartilaginous endplate has not yet fully fused to the vertebral bodies it is possible that the specimens tested may have been at an increased risk for this injury, although this mechanism of failure was only observed in the 300% neutral zone posture conditions with peak compressive loads of 40% UCT.

This investigation represents one of the first efforts to pair *in vitro* biomechanical testing with histological staining methods to characterize the combined influence of various exposure variables that have previously been linked to low back injury. However, there are a several potential limitations that should be addressed. First, the application of the findings from this study is limited by the use of porcine cervical FSUs, combined with the absence of any physiological repair mechanisms, as seen *in vivo*. However, previous research has confirmed anatomical and functional similarities (Oxland et al., 1991; Yingling et al., 1999) between the porcine cervical spine and the human lumbar spine; providing superior control over potential confounding factors (e.g. age, nutrition, physical activity) for *in vitro* biomechanics studies. Although the repair processes initiated by micro-damage in living

tissues cannot be simulated in an *in vitro* experiment, previous research has contended that the 5000 loading cycles may easily accumulate *in vivo* within two weeks of manual work or industrial exposure (Brinckmann et al., 1988). Moreover, Lotz et al. (1998) have demonstrated that murine intervertebral discs exposed to one week of static compression failed to fully recover 1 month after the loading protocol was ceased. This suggests that the accumulation of damage would likely exceed the rate of repair in both the IVD and cartilaginous endplate for the accelerated loading protocol that was examined in the present study.

The results presented in this study are also limited by the non-destructive method that was used to approximate the UCT of FSUs included in the study, which is based on approximating the intact intervertebral joint surface area using the equation of an ellipse to estimate failure force (Parkinson et al., 2005). This approach may not be suitable for human specimens, where a wide range of bone mineral density in the lumber vertebrae would be expected. In addition, our histological analyses are limited by the use of frontal and transverse sectioning planes to characterize the micro-structural damage imposed to the intra- and inter-lamellar matrix of the AF. Previous research conducted by Schollum et al. (2008) has demonstrated that oblique sectioning planes along the collagen fibre angle was highly effective for characterizing the complexity of the inter-lamellar architecture of the AF.

Lastly, although the cumulative compressive load dose applied to specimens varied across 10, 20 and 40% UCT individual loading cycles, it was balanced for all three cycle rates investigated. However, this

Fig. 4. Representative images illustrating baseline micro-structural damage in control specimens that were not subjected to cyclic compressive loading. Images shown were obtained from the posterior–lateral region of the intervertebral disc of a c56 control specimen.
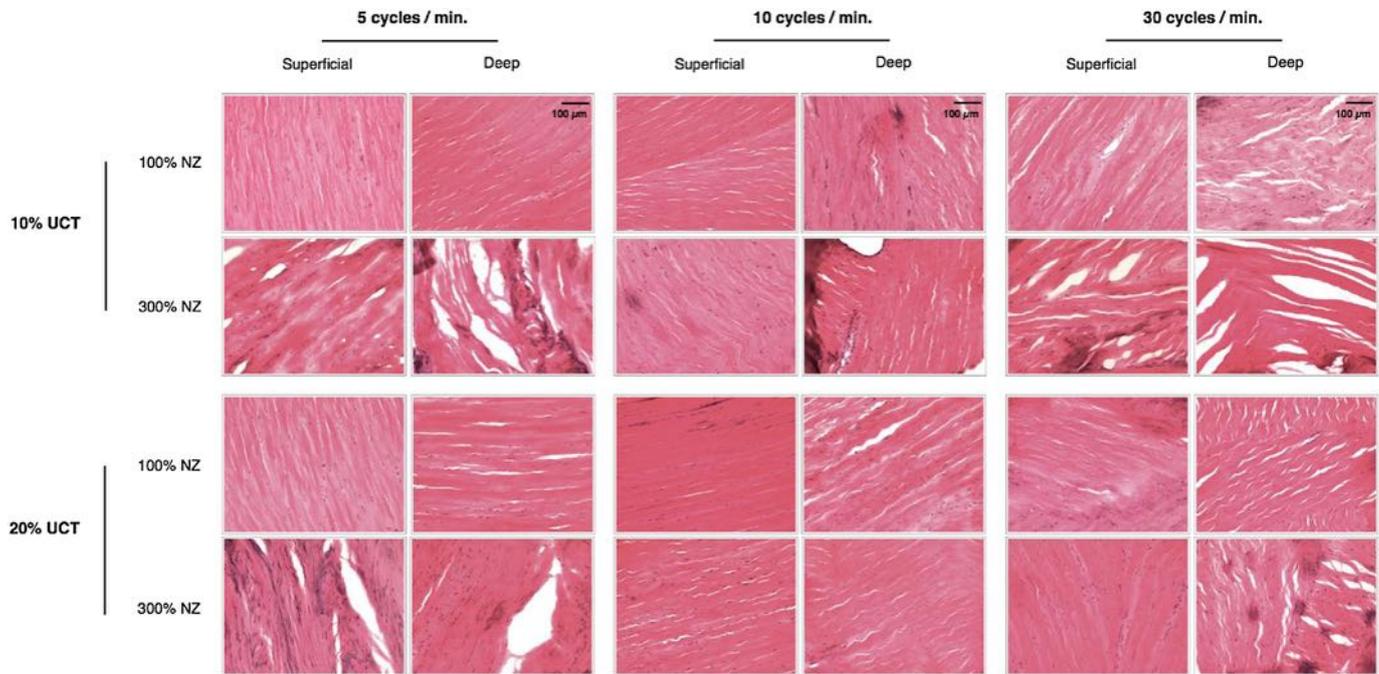
Fig. 5. Representative images of micro-structural damage in excised samples of annulus fibrosus tissue from the anterior region of the intervertebral disc (sectioned in the frontal plane) across experimental conditions. (UCT = ultimate compressive tolerance; NZ = neutral zone).

meant that that cyclic compressive loading protocol was applied over different test durations, ranging from 16 h and 40 min (5 cycles per minute) to 2 h and 47 min (30 cycles per minute). Despite best efforts to maintain consistent hydration across loading conditions, we did noticed that some specimens assigned to the 5 cycles per minute loading groups appeared more dehydrated while excising tissue samples for histological analysis. This may explain the trend of reduced survival and increased AF tissue disruption for specimens loaded at a rate of 5 cycles per minute, which contradicts the basic theory that more rest between cycles is generally considered to be protective.

5. Conclusion

Consistent with previous research, our findings support a threshold of peak compressive force of 30% UCT, where cyclic loading above this level will likely lead to fatigue injury of the cartilaginous endplate in less than 5000 cycles of *in vitro* mechanical loading. However, results from our histological analyses show that considerable IVD disruption occurred in specimens that "survived" 5000 cycles of cyclic loading at 10 and 20% UCT, with greater amounts of damage observed in the deeper layers of the AF. Research efforts are currently underway to
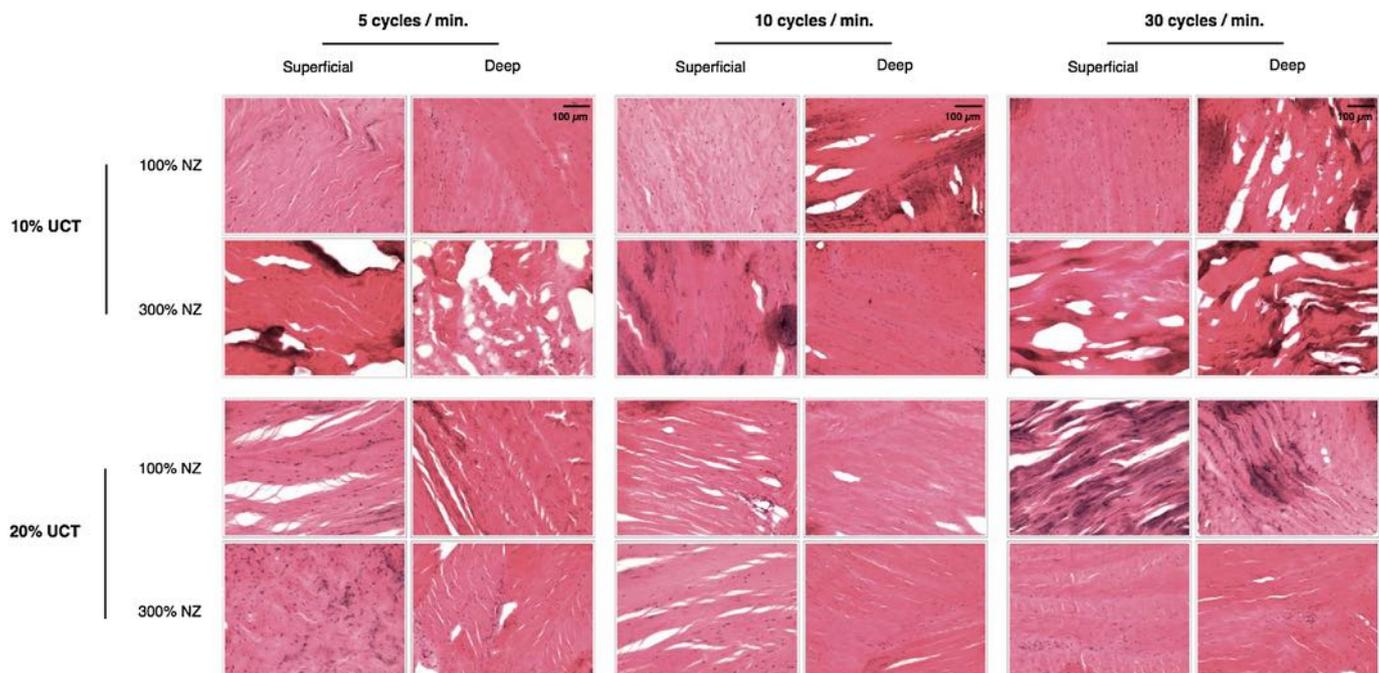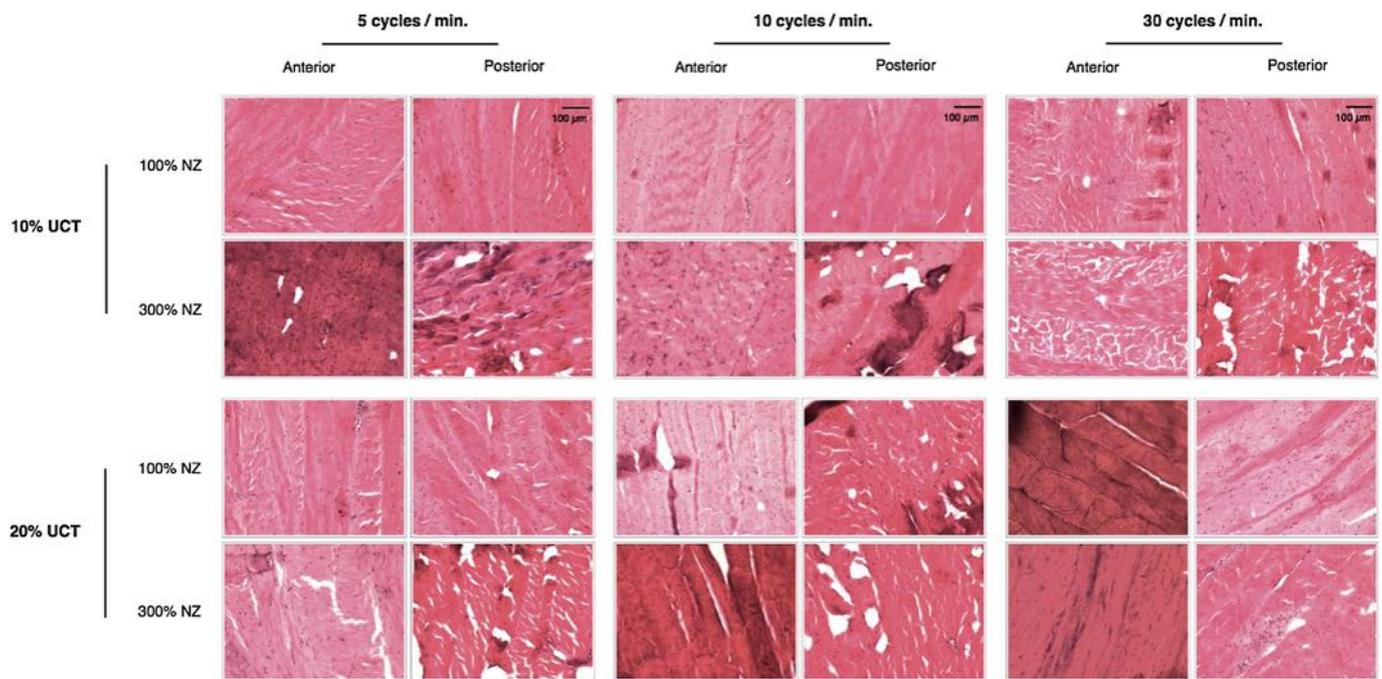

Fig. 6. Representative images of micro-structural damage in excised samples of annulus fibrosus tissue from the posterior–lateral region of the intervertebral disc (sectioned in the frontal plane) across experimental conditions. (UCT = ultimate compressive tolerance; NZ = neutral zone).

Fig. 7. Representative images of micro-structural damage in excised samples of annulus fibrosus tissue of the intervertebral disc (sectioned in the transverse plane) across experimental conditions. (UCT = ultimate compressive tolerance; NZ = neutral zone).

quantify differences in the amount of micro-structural damage across experimental conditions (i.e., size of clefts, density of disruption, etc.), as well characterize the relationship between the number of loading cycles and the accumulation of micro-structural disruption in the AF after set intervals of controlled exposure.

References

Adams, M.A., Hutton, W.C., 1983. The effect of fatigue on the lumbar intervertebral disc. J. Bone Joint Surg. Br. Vol. 65 (2), 199–203.

Brinckmann, M.P., Hilweg, D., 1989. Prediction of the compressive strength of human lumbar vertebrae. Clin. Biomech. 4 (S2), iii–27.

Brinckmann, P., Biggemann, M., Hilweg, D., 1988. Fatigue fracture of human lumbar vertebrae. Clin. Biomech. 3 (S1), i–S23.

Callaghan, J.P., McGill, S.M., 2001. Intervertebral disc herniation: studies on a porcine model exposed to highly repetitive flexion/extension motion with compressive force. Clin. Biomech. 16 (1), 28–37.

Coenen, P., Kingma, I., Boot, C.R., Twisk, J.W., Bongers, P.M., van Dieën, J.H., 2013. Cumulative low back load at work as a risk factor of low back pain: a prospective cohort study. J. Occup. Rehabil. 23 (1), 11–18.

Denis, F., Burkus, J.K., 1992. Shear fracture-dislocations of the thoracic and lumbar spine associated with forceful hyperextension (lumberjack paraplegia). Spine 17 (2), 156–161.

Galante, J.O., 1967. Tensile properties of the human lumbar annulus fibrosus. Acta Orthop. Scand. Suppl. 100, 1–91.

Gallagher, S., Marras, W.S., Litsky, A.S., Burr, D., 2005. Torso flexion loads and the fatigue failure of human lumbosacral motion segments. Spine 30 (20), 2265–2273.

Gooyers, C.E., Frost, D.M., McGill, S.M., Callaghan, J.P., 2013. Partial rupture of the Achilles tendon during a simulated fire ground task: insights obtained from a case report for the prevention and reporting of musculoskeletal injury. Clin. Biomech. 28 (4), 436–440.

Hansson, T.H., Keller, T.S., Spengler, D.M., 1987. Mechanical behavior of the human lumbar spine. II. Fatigue strength during dynamic compressive loading. J. Orthop. Res. 5 (4), 479–487.

Howarth, S.J., Callaghan, J.P., 2013. Towards establishing an occupational threshold for cumulative shear force in the vertebral joint - an in vitro evaluation of a risk factor for spondylolytic fractures using porcine specimens. Clin. Biomech. 28 (3), 246–254.

Kaplan, E.L., Meier, P., 1958. Nonparametric estimation from incomplete observations. J. Am. Stat. Assoc. 53 (282), 457–481.

Kumar, S., 1990. Cumulative load as a risk factor for back pain. Spine 15 (12), 1311–1316.

Liu, Y.K., Njus, G., Buckwalter, J., Wakano, K., 1983. Fatigue response of lumbar intervertebral joints under axial cyclic loading. Spine 8 (8), 857.

Lotz, J.C., Colliou, O.K., Chin, J.R., Duncan, N.A., Liebenberg, E., 1998. Compression-induced degeneration of the intervertebral disc: an in vivo mouse model and finite-element study. Spine 23 (23), 2493–2506.

Norman, R., Wells, R., Neumann, P., Frank, J., Shannon, H., Kerr, M., 1998. A comparison of peak vs cumulative physical work exposure risk factors for the reporting of low back pain in the automotive industry. Clin. Biomech. 13 (8), 561–573.

Oxland, T.R., Panjabi, M.M., Southern, E.P., Duranceau, J.S., 1991. An anatomic basis for spinal instability: a porcine trauma model. J. Orthop. Res. 9 (3), 452–462.

Parkinson, R.J., Callaghan, J.P., 2007a. Can periods of static loading be used to enhance the resistance of the spine to cumulative compression? J. Biomech. 40 (13), 2944–2952.

Parkinson, R.J., Callaghan, J.P., 2007b. The role of load magnitude as a modifier of the cumulative load tolerance of porcine cervical spinal units: progress towards a force weighting approach. Theor. Issues Econ. Sci. 8 (3), 171–184.

Parkinson, R.J., Callaghan, J.P., 2008. Quantification of the relationship between load magnitude, rest duration and cumulative compressive tolerance of the spine: development of a weighting system for adjustment to a common injury exposure level. Theor. Issues Econ. Sci. 9 (3), 255–268.

Parkinson, R.J., Callaghan, J.P., 2009. The role of dynamic flexion in spine injury is altered by increasing dynamic load magnitude. Clin. Biomech. 24 (2), 148–154.

Parkinson, R.J., Durkin, J.L., Callaghan, J.P., 2005. Estimating the compressive strength of the porcine cervical spine: an examination of the utility of DXA. Spine 30 (17), E492–E498.

Parkinson, R.J., Bezaire, M., Callaghan, J.P., 2011. A comparison of low back kinetic estimates obtained through posture patching, rigid link modeling and an EMG-assisted model. Appl. Ergon. 42 (5), 644–651.

Schollum, M.L., Robertson, P.A., Broom, N.D., 2008. ISSLS prize winner: microstructure and mechanical disruption of the lumbar disc annulus. Part I: a microscopic investigation of the translamellar bridging network. Spine 33 (25), 2702–2710.

Seidler, A., 2001. The role of cumulative physical work load in lumbar spine disease: risk factors for lumbar osteochondrosis and spondylosis associated with chronic complaints. Occup. Environ. Med. 58 (11), 735–746.

Seidler, A., 2003. Occupational risk factors for symptomatic lumbar disc herniation; a case–control study. Occup. Environ. Med. 60 (11), 821–830.

Standaert, C.J., Herring, S.A., 2000. Spondylolysis: a critical review. Br. J. Sports Med. 34 (6), 415–422.

Tampier, C., Drake, J.D., Callaghan, J.P., McGill, S.M., 2007. Progressive disc herniation: an investigation of the mechanism using radiologic, histochemical, and microscopic dissection techniques on a porcine model. Spine 32 (25), 2869–2874.

Thompson, R.E., Barker, T.M., Pearcy, M.J., 2003. Defining the neutral zone of sheep intervertebral joints during dynamic motions: an in vitro study. Clin. Biomech. 18 (2), 89–98.

Wade, K.R., Roertson, P.A., Thambyah, A., Broom, N.D., 2014. How Healthy Discs Herniate. A biomechanical and microstructural study investigating the combines effects of compression rate and flexion. Spine 39 (13), 1018–1028.

Yingling, V.R., Callaghan, J.P., McGill, S.M., 1997. Dynamic loading affects the mechanical properties and failure site of porcine spines. Clin. Biomech. 12 (5), 301–305.

Yingling, V.R., Callaghan, J.P., McGill, S.M., 1999. The porcine cervical spine as a model of the human lumbar spine: an anatomical, geometric, and functional comparison. J. Spinal Disord. 12 (6), 501–508.